SOI: 1.1/TAS DOI: 10.15863/TAS
International Scientific Journal
Theoretical & Applied Science

p-ISSN: 2308-4944 (print) **e-ISSN:** 2409-0085 (online)

Year: 2021 **Issue:** 12 **Volume:** 104

Published: 21.12.2021 http://T-Science.org

QR – Issue QR – Article

Denis Chemezov
Vladimir Industrial College
M.Sc.Eng., Corresponding Member of International Academy of Theoretical and Applied Sciences, Lecturer, Russian Federation
https://orcid.org/0000-0002-2747-552X
vic-science@yandex.ru

Aleksey Kuznetsov
Vladimir Industrial College
Student, Russian Federation

Georgiy Karatun
Vladimir Industrial College
Student, Russian Federation

Irina Pavlukhina
Vladimir Industrial College
Lecturer, Russian Federation

Andrey Karasyov
Vladimir Industrial College
Student, Russian Federation

Maksim Perov
Vladimir Industrial College
Student, Russian Federation

Andrey Tyulkin
Vladimir Industrial College
Student, Russian Federation

REFERENCE DATA OF PRESSURE DISTRIBUTION ON THE SURFACES OF AIRFOILS HAVING THE NAMES BEGINNING WITH THE LETTER C

***Abstract**: The results of the computer calculation of air flow around the airfoils having the names beginning with the letter C are presented in the article. The contours of pressure distribution on the surfaces of the airfoils at the angles of attack of 0, 15 and -15 degrees in conditions of the subsonic airplane flight speed were obtained.*

***Key words**: the airfoil, the angle of attack, pressure, the surface.*
***Language**: English*
***Citation**: Chemezov, D., et al. (2021). Reference data of pressure distribution on the surfaces of airfoils having the names beginning with the letter C. *ISJ Theoretical & Applied Science, 12 (104)*, 814-844.
Soi: http://s-o-i.org/1.1/TAS-12-104-86 ***Doi***: crossref https://dx.doi.org/10.15863/TAS.2021.12.104.86
***Scopus ASCC**: 1507.*

Introduction

Creating reference materials that determine the most accurate pressure distribution on the airfoils surfaces is an actual task of the airplane aerodynamics.

Materials and methods

The study of air flow around the airfoils was carried out in a two-dimensional formulation by means of the computer calculation in the *Comsol Multiphysics* program.

The airfoils in the cross section were taken as objects of research [1-14]. In this work, the airfoils having the names beginning with the letter *C* were adopted. Air flow around the airfoils was carried out at the angles of attack (α) of 0, 15 and -15 degrees.

The flight speed of the airplane in each case was subsonic. The airplane flight in the atmosphere was carried out under normal weather conditions. The geometric characteristics of the studied airfoils are presented in the Table 1. The studied geometric shapes of the airfoils in the cross section are presented in the Table 2.

Table 1. The geometric characteristics of the airfoils.

Airfoil name	Max. thickness	Max. camber	Leading edge radius	Trailing edge thickness
C72	11.73% at 30.0% of the chord	5.87% at 30.0% of the chord	1.3308%	0.1%
CAGI 731	10.06% at 30.0% of the chord	2.42% at 30.0% of the chord	1.3983%	0.0%
CAGID2	9.97% at 30.0% of the chord	2.88% at 20.0% of the chord	1.006%	0.0%
cap 21	15.59% at 15.7% of the chord	0.62% at 23.9% of the chord	3.2138%	0.0%
CAST 10-2/DOA 2 transonic airfoil	12.18% at 45.6% of the chord	1.54% at 69.5% of the chord	0.9165%	0.5%
Cavini 15	11.7% at 30.0% of the chord	5.85% at 30.0% of the chord	1.1643%	0.0%
CH10 (smoothed)	12.84% at 30.6% of the chord	10.2% at 49.3% of the chord	1.2557%	0.011%
Cheesman 25-1,00-10	10.1% at 25.0% of the chord	6.7% at 50.0% of the chord	1.5944%	0.0%
CHEN	12.44% at 26.6% of the chord	7.76% at 26.6% of the chord	1.9015%	0.0%
Chen high lift airfoil	12.44% at 26.6% of the chord	7.76% at 26.6% of the chord	1.8978%	0.0%
CJ 1	9.5% at 30.0% of the chord	1.25% at 30.0% of the chord	1.2343%	0.3%
CJ 2	5.6% at 20.0% of the chord	2.3% at 30.0% of the chord	0.7868%	0.25%
CJ 3309	9.2% at 30.0% of the chord	3.4% at 30.0% of the chord	0.7862%	0.2%
CJ 4	13.7% at 30.0% of the chord	2.35% at 30.0% of the chord	1.3037%	0.6%
CJ 5	9.3% at 20.0% of the chord	2.3% at 30.0% of the chord	1.137%	0.0%
CJ 6	5.6% at 20.0% of the chord	2.3% at 30.0% of the chord	0.7868%	0.25%
CJ25209	9.5% at 25.4% of the chord	2.5% at 25.4% of the chord	0.6116%	0.0%
CJ-25209	9.31% at 30.0% of the chord	2.47% at 20.0% of the chord	0.7841%	0.1%
CJ-3209	9.34% at 30.0% of the chord	1.98% at 30.0% of the chord	0.8173%	0.0%
CJ-3406	6.0% at 20.0% of the chord	4.0% at 30.0% of the chord	0.7%	0.2%
CLARK K	11.69% at 30.1% of the chord	3.26% at 40.1% of the chord	1.9382%	0.12%
CLARK V	11.64% at 30.0% of the chord	3.42% at 50.0% of the chord	1.1512%	0.14%
CLARK W	11.22% at 30.0% of the chord	3.76% at 40.0% of the chord	1.4457%	0.1%
CLARK X	11.7% at 30.0% of the chord	3.3% at 40.0% of the chord	1.2523%	0.12%
CLARK Y	11.71% at 28.0% of the chord	3.43% at 42.0% of the chord	1.0714%	0.1199%
CLARK YH	11.9% at 30.0% of the chord	5.95% at 30.0% of the chord	1.8596%	0.1%
CLARK YH- Mod,	8.33% at 30.0% of the chord	5.95% at 30.0% of the chord	1.5909%	0.07%
CLARK YM-15	14.98% at 30.1% of the chord	3.55% at 40.1% of the chord	2.0202%	0.16%
CLARK YM-18	17.98% at 30.2% of the chord	3.55% at 40.2% of the chord	2.884%	0.18%
CLARK YS	11.7% at 30.0% of the chord	2.35% at 30.0% of the chord	1.2661%	0.0%
CLARK Z	11.75% at 30.0% of the chord	4.06% at 40.0% of the chord	1.6416%	0.12%
CLARK-Y 11,7% smoothed	11.72% at 30.9% of the chord	3.55% at 43.5% of the chord	1.2361%	0.0%
CLARKY15	15.0% at 30.0% of the chord	5.85% at 30.0% of the chord	1.9854%	0.16%
CLARKY18	18.0% at 30.0% of the chord	5.85% at 30.0% of the chord	2.831%	0.18%
CLARK-Y2	11.7% at 30.9% of the chord	3.58% at 40.2% of the chord	1.1426%	0.0%
CLARKYSimm	18.33% at 36.0% of the chord	0.0% at 0.0% of the chord	0.7217%	0.12%
Coanda 2	6.0% at 30.0% of the chord	4.3% at 30.0% of the chord	0.6871%	0.0%
COANDA-1	5.65% at 30.0% of the chord	4.17% at 30.0% of the chord	0.6522%	0.0%
COANDA-3	7.0% at 30.0% of the chord	4.2% at 30.0% of the chord	0.6242%	0.0%
CONA	10.0% at 31.3% of the chord	2.96% at 31.3% of the chord	0.3463%	0.258%
CR 001	7.33% at 27.1% of the chord	4.06% at 45.4% of the chord	0.5493%	0.001%
cr001sm	7.33% at 27.1% of the chord	4.06% at 45.4% of the chord	0.5493%	0.001%
CRD-1	7.62% at 30.0% of the chord	7.13% at 50.0% of the chord	1.0378%	0.7%
CRD-2	6.59% at 30.0% of the chord	6.57% at 50.0% of the chord	0.8749%	0.65%
CRD-3	6.85% at 30.0% of the chord	7.3% at 50.0% of the chord	0.8364%	0.75%
CRD-4	5.36% at 20.0% of the chord	6.55% at 40.0% of the chord	0.7901%	0.6%
cristal cb85_15_7	15.69% at 40.0% of the chord	3.5% at 40.0% of the chord	0.8645%	0.0%

CSS	10.0% at 33.5% of the chord	4.85% at 35.5% of the chord	5.4407%	0.779%
Curtiss C 62	8.02% at 30.0% of the chord	1.92% at 40.0% of the chord	1.5114%	0.0%
Curtiss C 72	11.73% at 30.0% of the chord	5.87% at 30.0% of the chord	1.3308%	0.1%
CURTISS CR-1	12.21% at 24.0% of the chord	4.71% at 42.0% of the chord	1.399%	0.0035%

Note:
CAGI 731 (USSR);
Cavini 15 (L. Cavini (Italy));
CH10 (Chuch Hollinger CH 10-48-13 high lift low Reynolds number airfoil, smoothed);
Cheesman 25-1,00-10 (USA);
Chen high lift airfoil (University of Illinois);
CJ 1, CJ 2, CJ 4, CJ 5, CJ 6 (USA);
CJ 3309 (USA);
Coanda 2 (H. Coanda (Romania));
CR 001 (Cody Robertson CR 001 R/C hand-launch low Reynolds number airfoil (smoothed));
Curtiss C 62, Curtiss C 72 (G. Curtiss (USA));
CURTISS CR-1 (General aviation airfoil).

Table 2. The geometric shapes of the airfoils in the cross section.

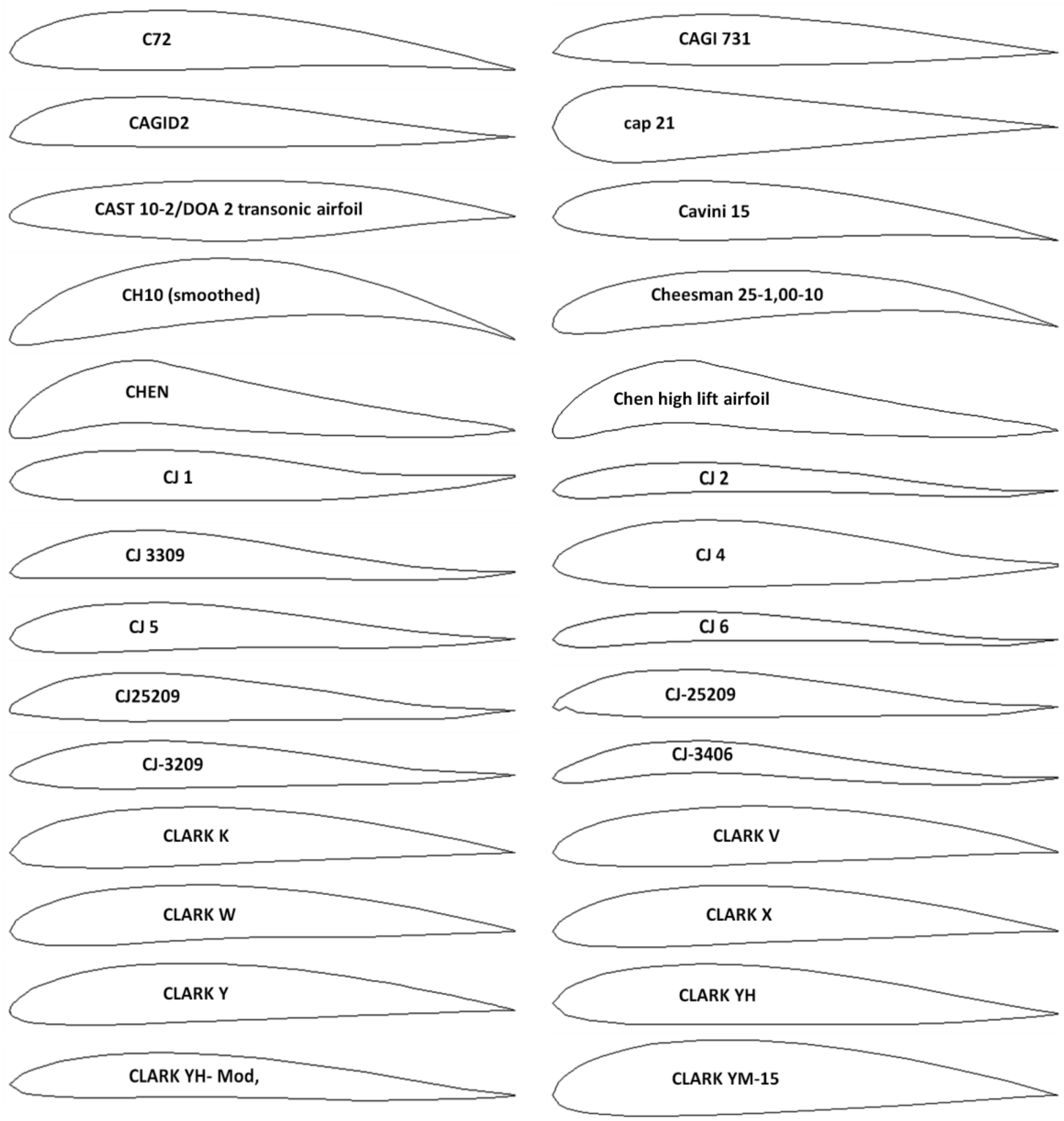

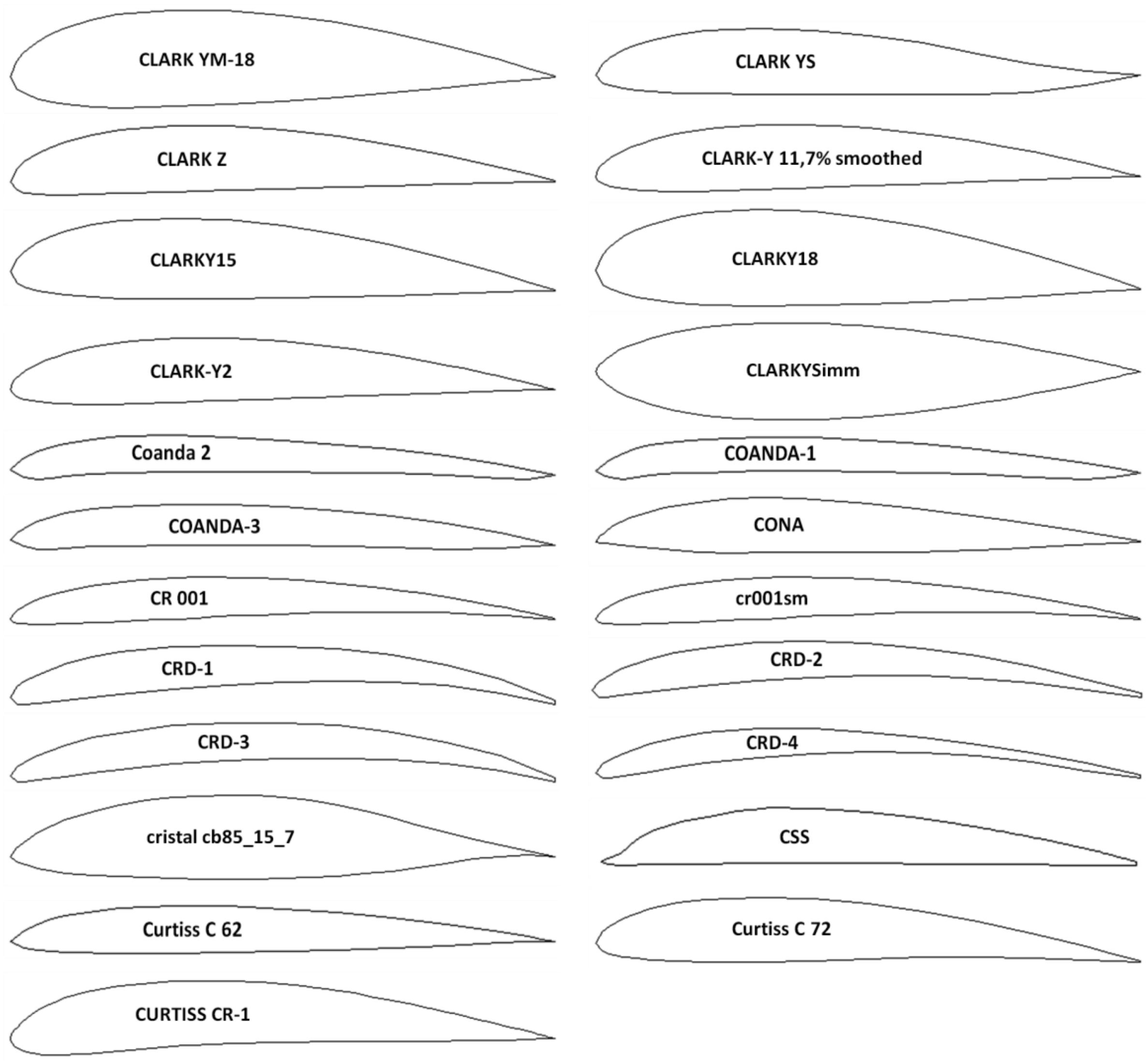

Results and discussion

The calculated pressure contours on the surfaces of the airfoils at the different angles of attack are presented in the Figs. 1-51.

The calculated magnitudes on the scale can be represented as the basic magnitudes when comparing the pressure drop under conditions of changing the angle of attack of the airfoils.

The optimal airfoil should have good aerodynamic characteristics, i.e. low drag and high lift. The modified version of the CHEN airfoil is subjected to less negative pressure at the different angles of attack. The pressure difference near the upper and lower surfaces of the CJ 2 airfoil is approximately 172 kPa, i.e. it varies by more than 20 times. This indicates a large lift of the airplane wing.

In conditions of the airplane's descent, maximum pressure of -180 kPa acts on the CJ 2 airfoil.

The CSS airfoil is subjected to a minimum pressure of -11.9 kPa at the similar negative angle of attack.

Changing the angle of attack of the Chen high lift airfoil to 15 degrees is accompanied by pressure of -19.2 kPa, which is the minimum pressure magnitude for all considered airfoils.

The minimum negative pressure magnitude was determined in conditions of horizontal flight of the airplane on the upper surface of the CAST 10-2/DOA 2 transonic airfoil. Also, the minimum drag magnitude at the leading edge was calculated for this airfoil. This indicates the most favorable conditions for the airplane flight.

During the airplane maneuvers, the leading edge of the airfoils is subjected to both positive and negative pressures.

The maximum increase in pressure on the leading edge occurs at the angle of attack of -15 degrees for some airfoils:

- CAST 10-2/DOA 2 transonic airfoil;
- Cheesman 25-1,00-10;
- CHEN, Chen high lift airfoil;
- CJ 1, CJ 2, CJ 4, CJ 5;

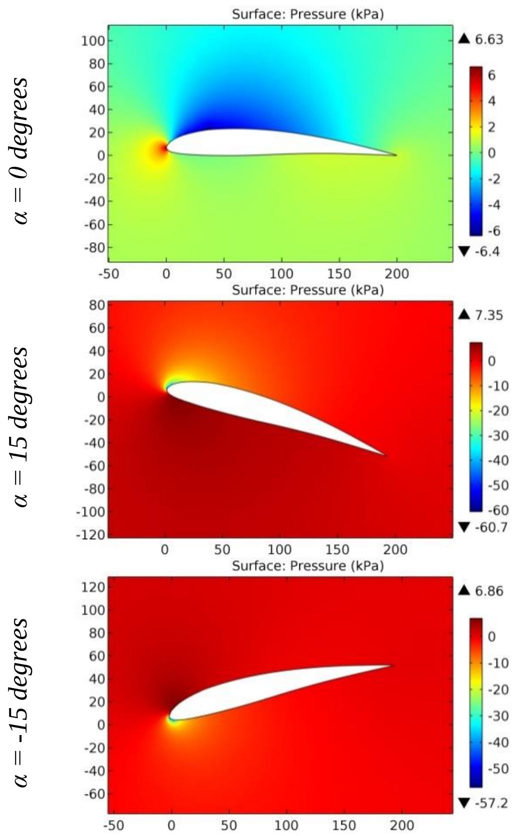

Figure 1. The pressure contours on the surfaces of the C72 airfoil.

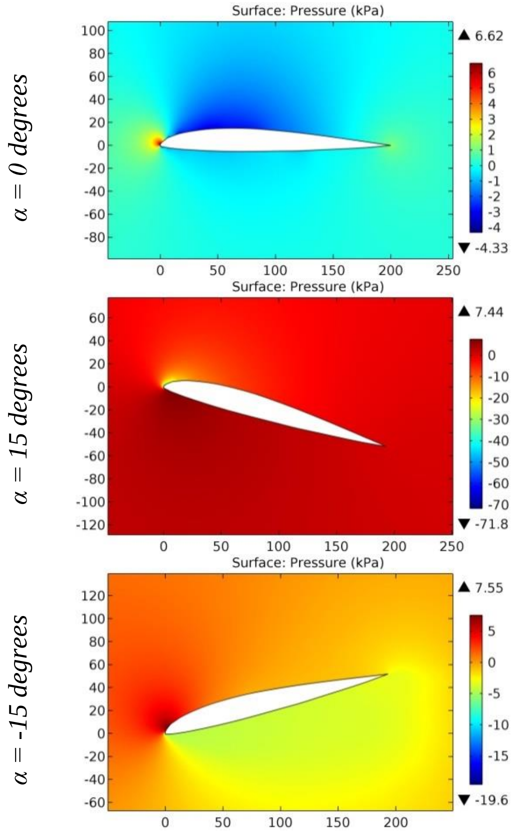

Figure 2. The pressure contours on the surfaces of the CAGI 731 airfoil.

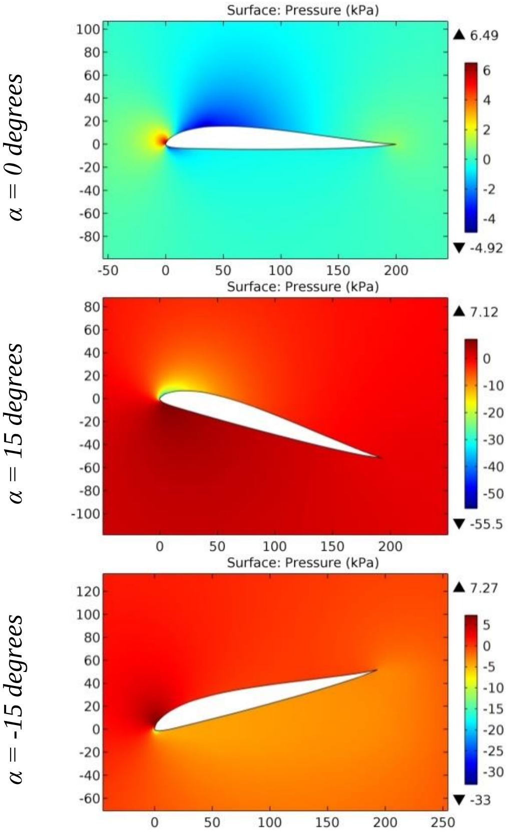

Figure 3. The pressure contours on the surfaces of the CAGID2 airfoil.

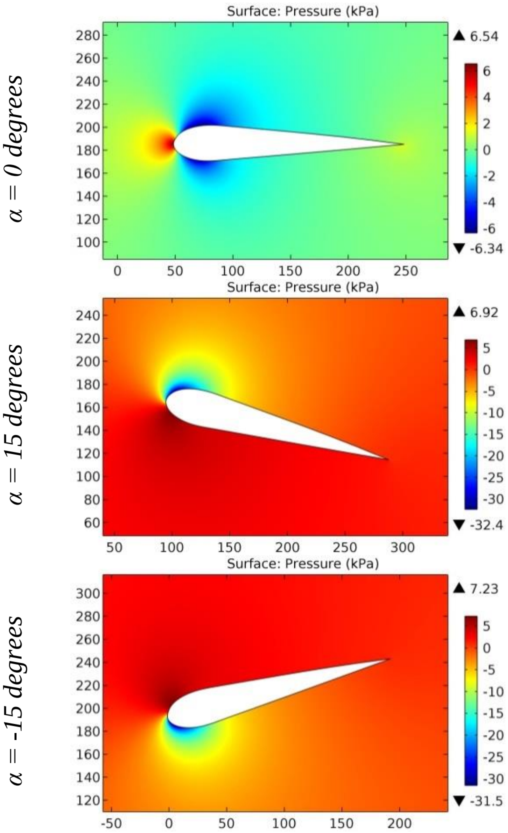

Figure 4. The pressure contours on the surfaces of the cap 21 airfoil.

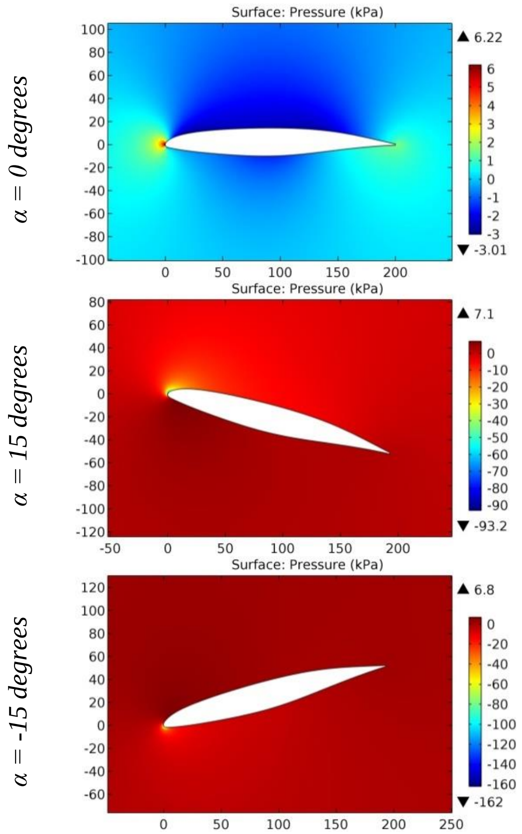

Figure 5. The pressure contours on the surfaces of the CAST 10-2/DOA 2 transonic airfoil.

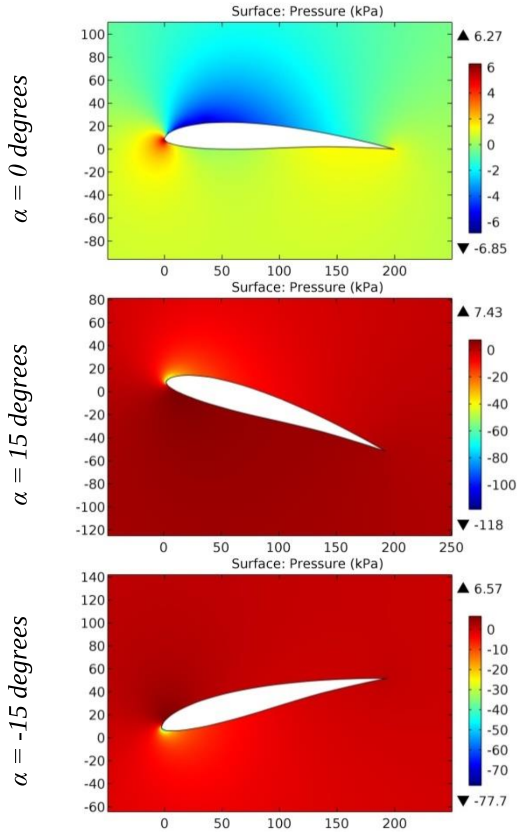

Figure 6. The pressure contours on the surfaces of the Cavini 15 airfoil.

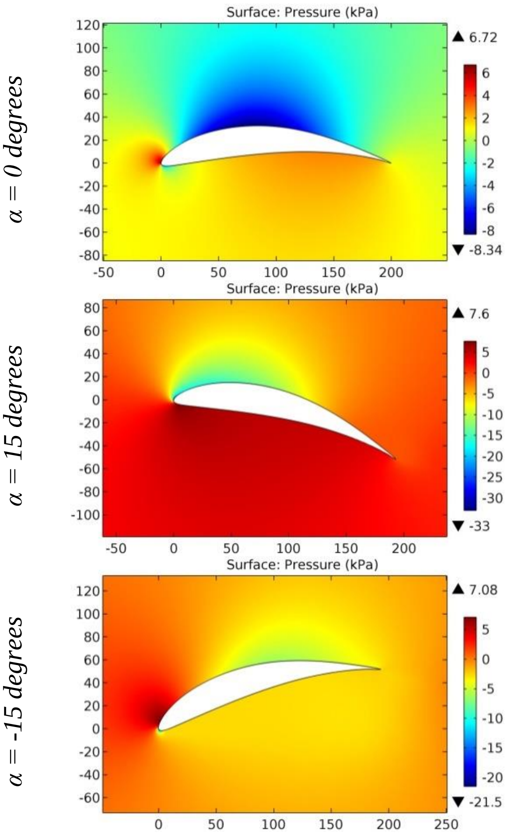

Figure 7. The pressure contours on the surfaces of the CH10 (smoothed) airfoil.

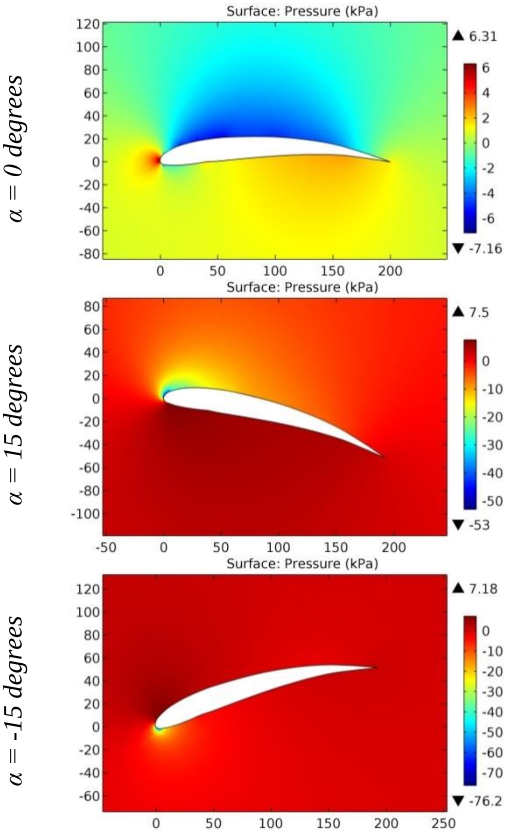

Figure 8. The pressure contours on the surfaces of the Cheesman 25-1,00-10 airfoil.

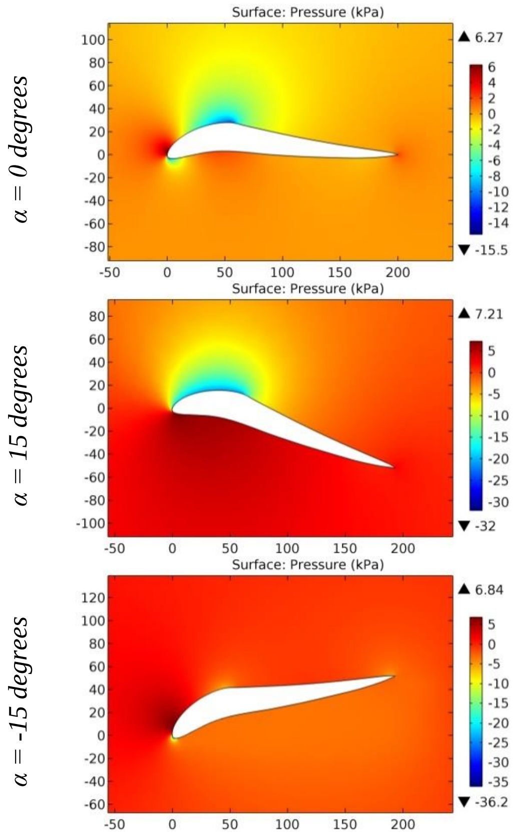

Figure 9. The pressure contours on the surfaces of the CHEN airfoil.

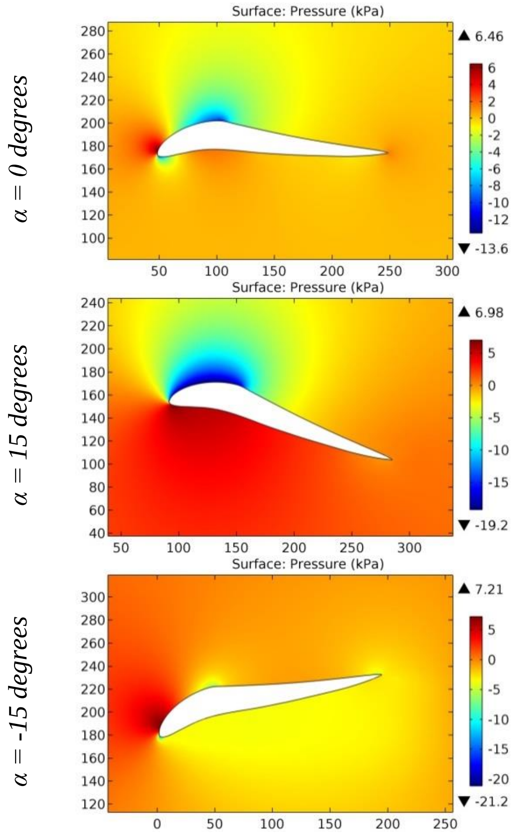

Figure 10. The pressure contours on the surfaces of the Chen high lift airfoil.

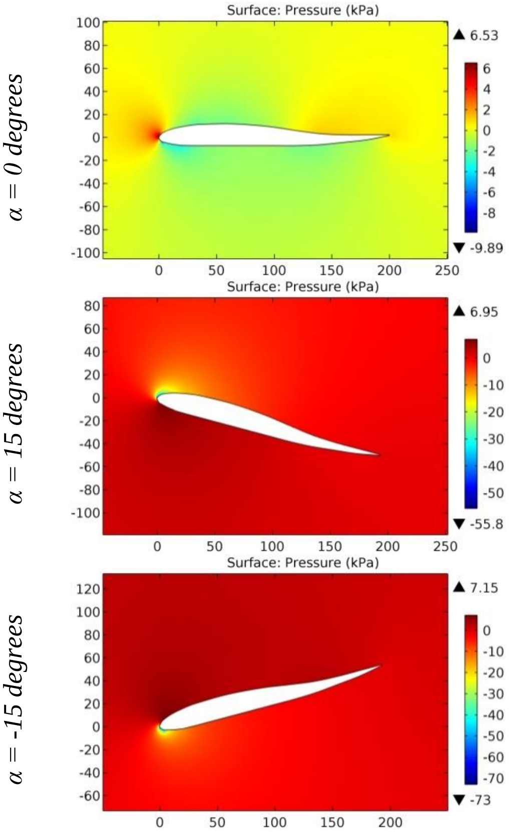

Figure 11. The pressure contours on the surfaces of the CJ 1 airfoil.

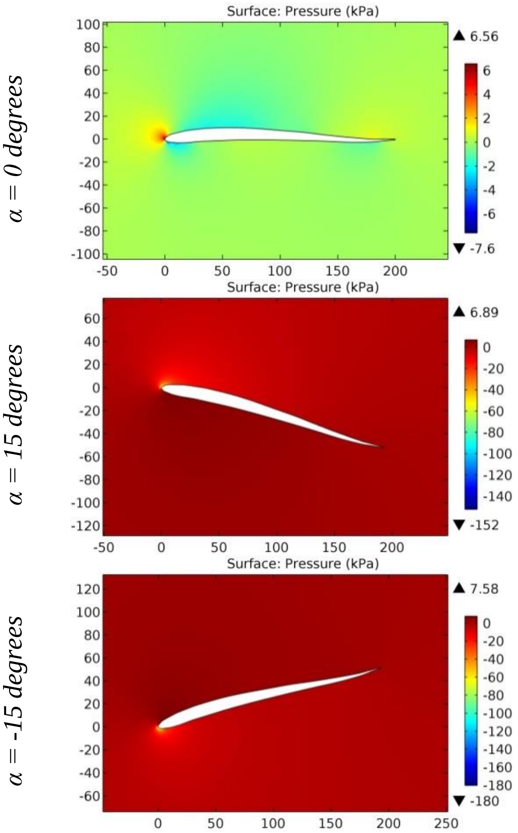

Figure 12. The pressure contours on the surfaces of the CJ 2 airfoil.

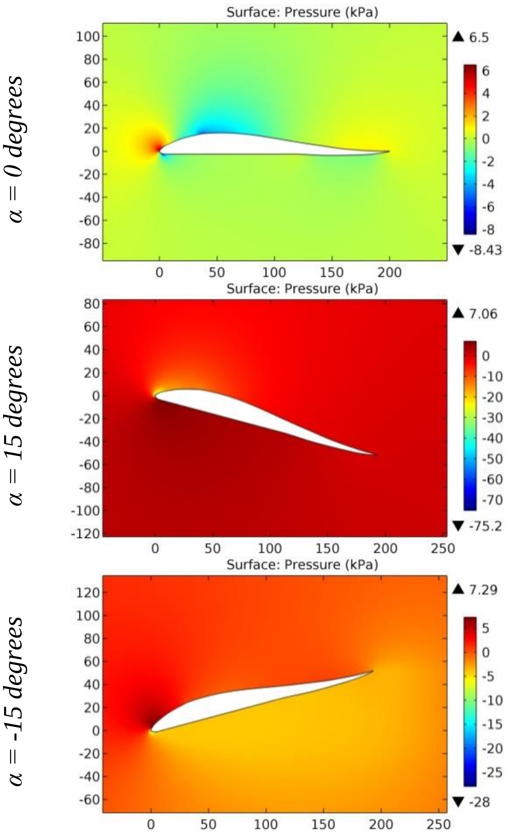

Figure 13. The pressure contours on the surfaces of the CJ 3309 airfoil.

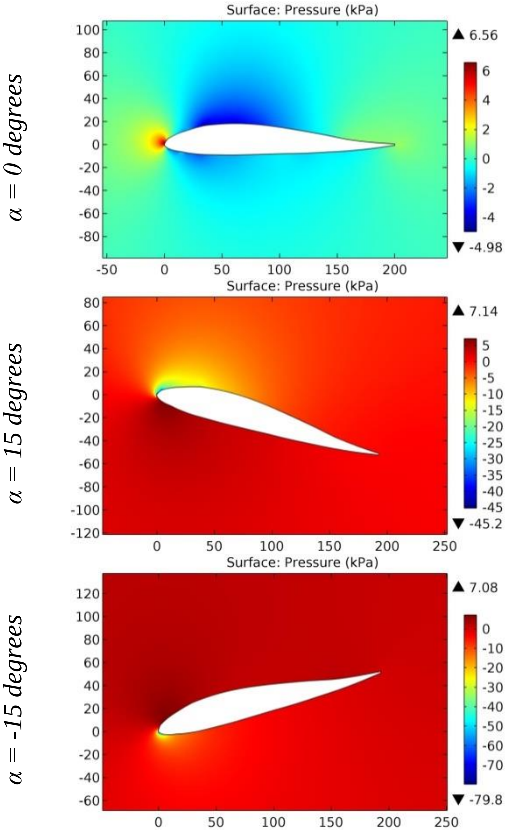

Figure 14. The pressure contours on the surfaces of the CJ 4 airfoil.

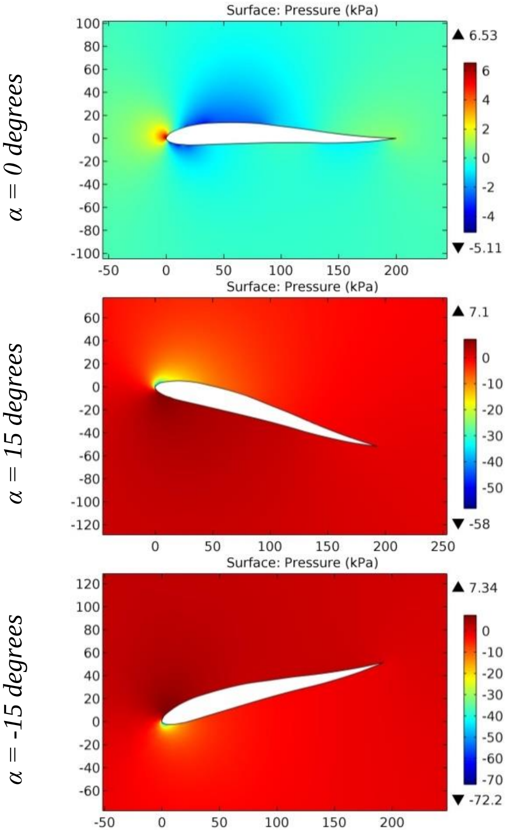

Figure 15. The pressure contours on the surfaces of the CJ 5 airfoil.

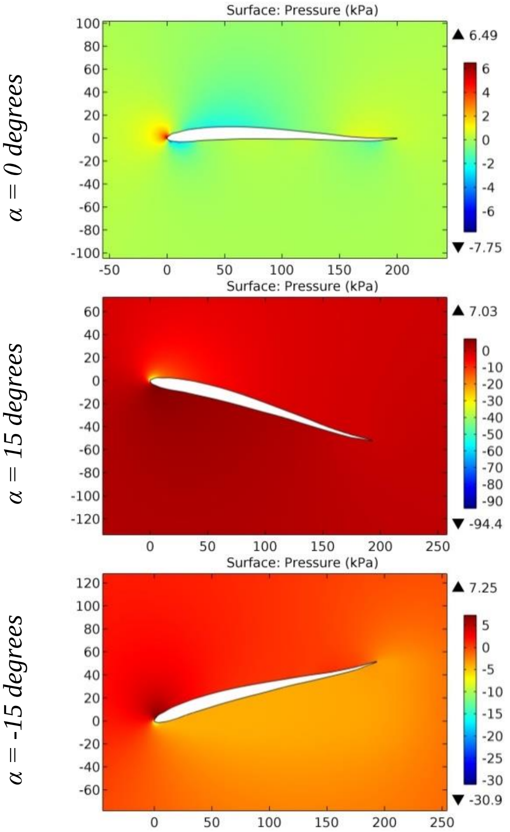

Figure 16. The pressure contours on the surfaces of the CJ 6 airfoil.

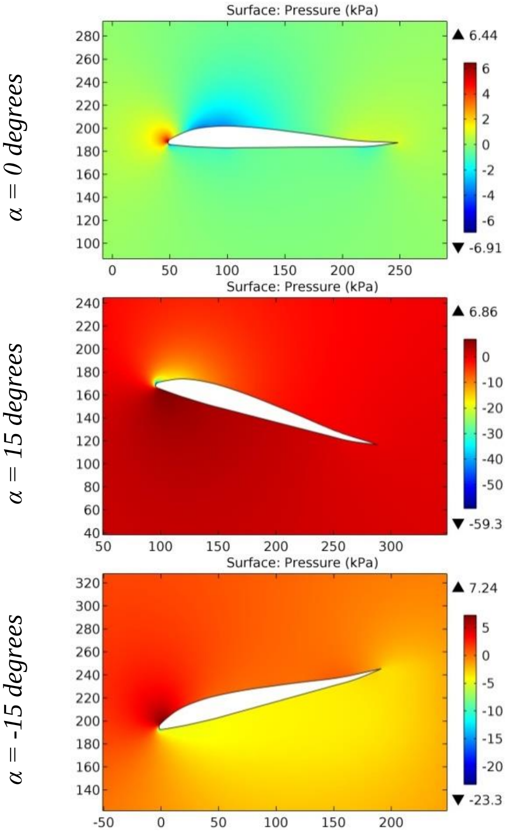

Figure 17. The pressure contours on the surfaces of the CJ25209 airfoil.

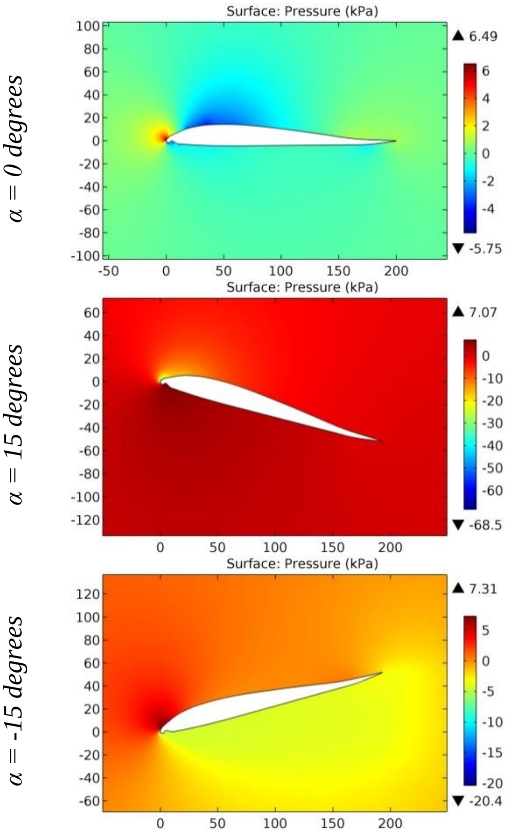

Figure 18. The pressure contours on the surfaces of the CJ-25209 airfoil.

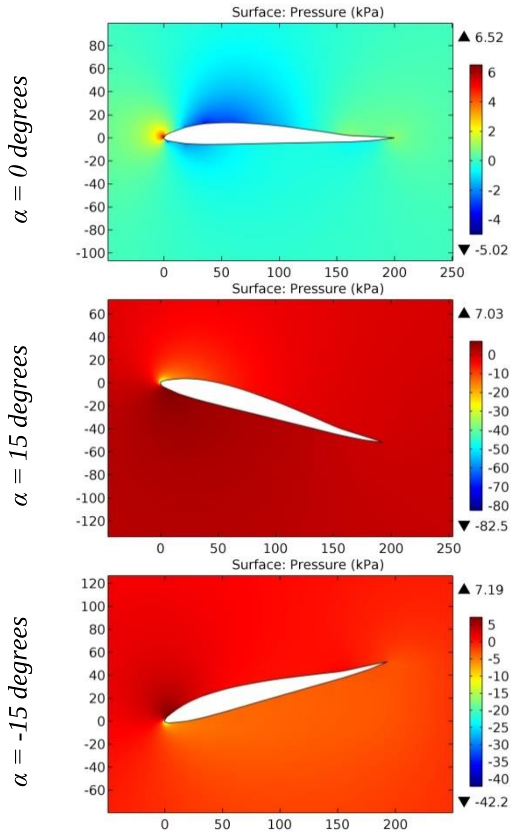

Figure 19. The pressure contours on the surfaces of the CJ-3209 airfoil.

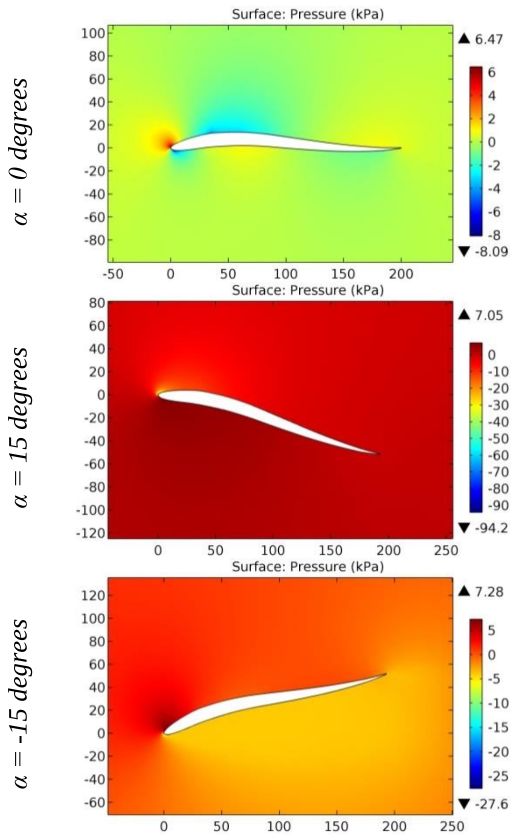

Figure 20. The pressure contours on the surfaces of the CJ-3406 airfoil.

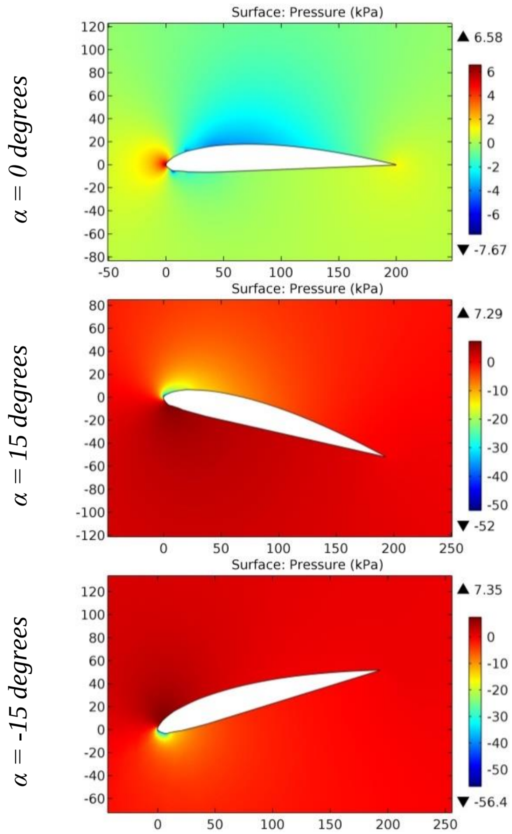

Figure 21. The pressure contours on the surfaces of the CLARK K airfoil.

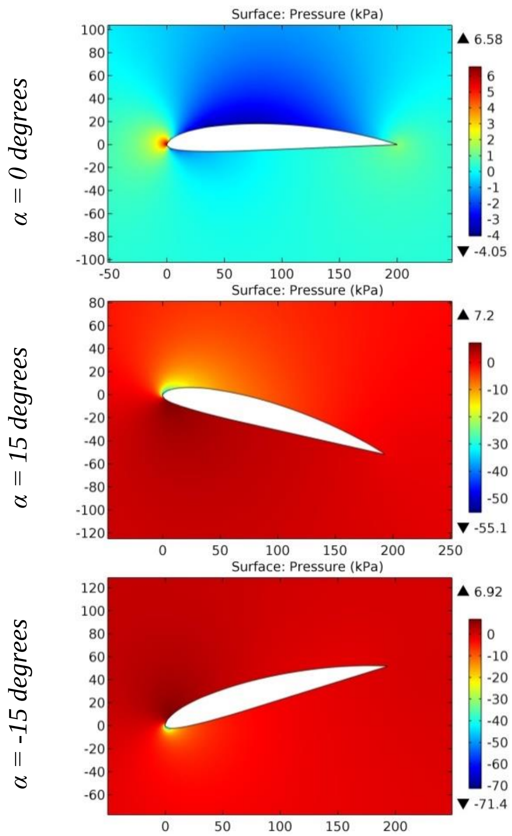

Figure 22. The pressure contours on the surfaces of the CLARK V airfoil.

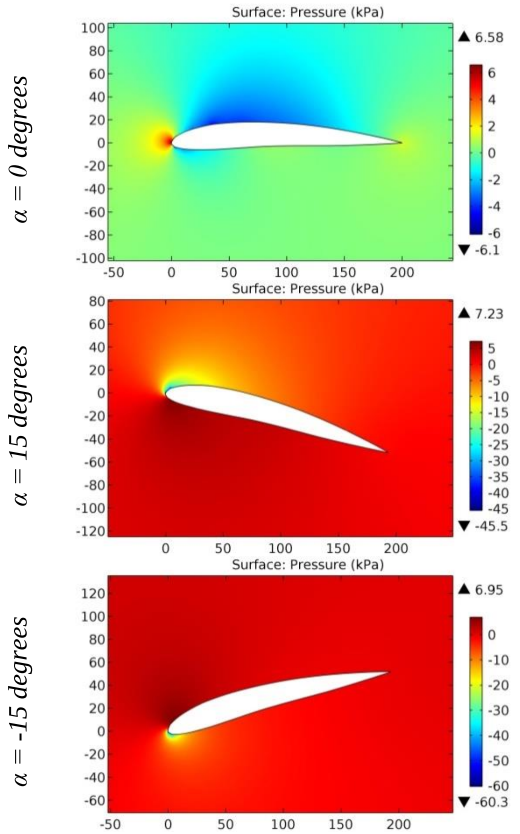

Figure 23. The pressure contours on the surfaces of the CLARK W airfoil.

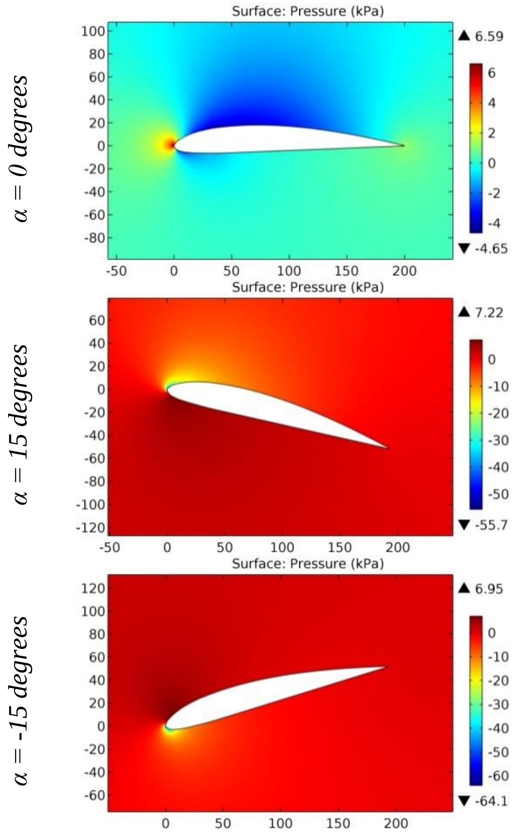

Figure 24. The pressure contours on the surfaces of the CLARK X airfoil.

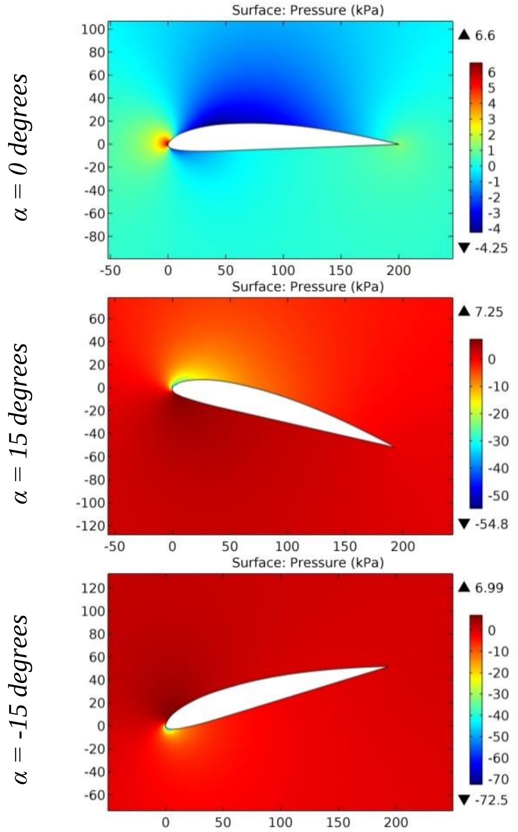

Figure 25. The pressure contours on the surfaces of the CLARK Y airfoil.

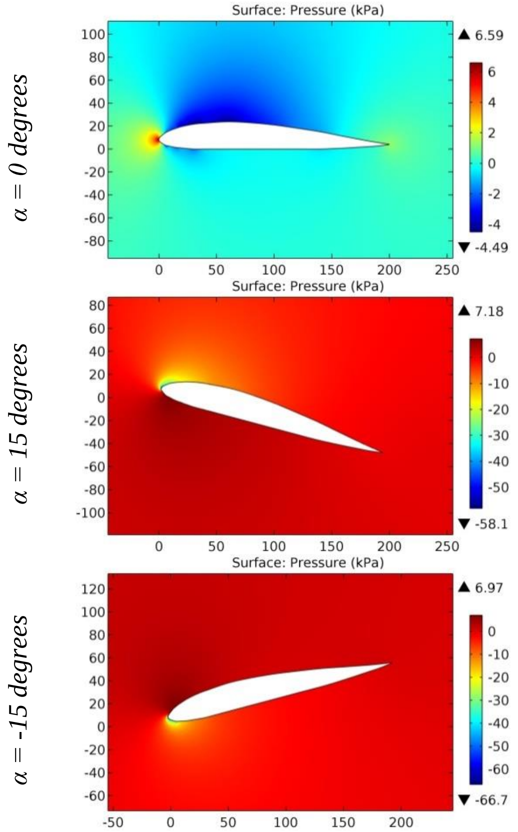

Figure 26. The pressure contours on the surfaces of the CLARK YH airfoil.

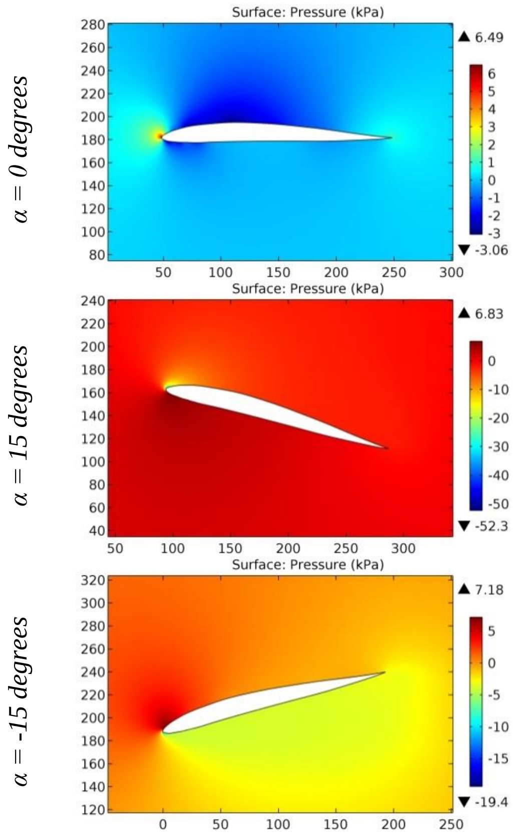

Figure 27. The pressure contours on the surfaces of the CLARK YH- Mod airfoil.

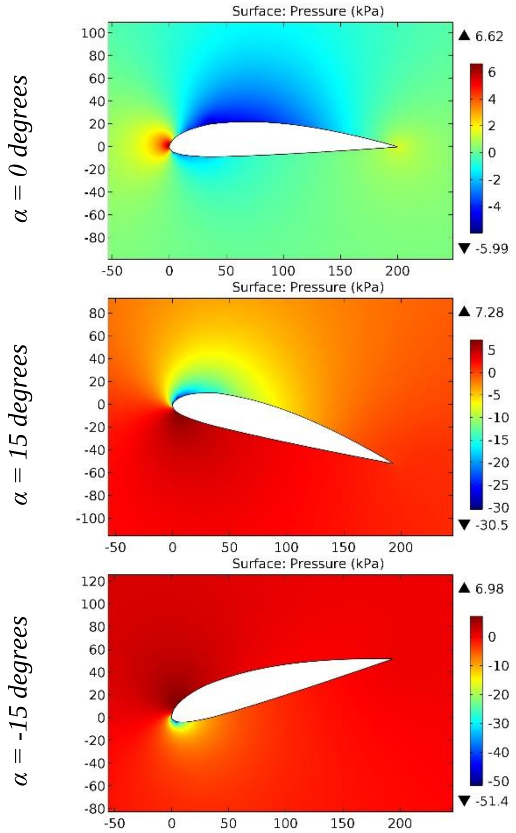

Figure 28. The pressure contours on the surfaces of the CLARK YM-15 airfoil.

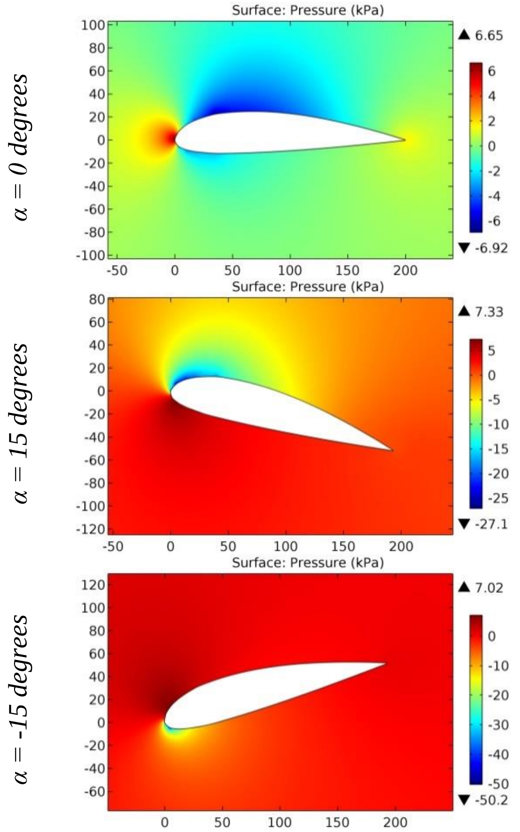

Figure 29. The pressure contours on the surfaces of the CLARK YM-18 airfoil.

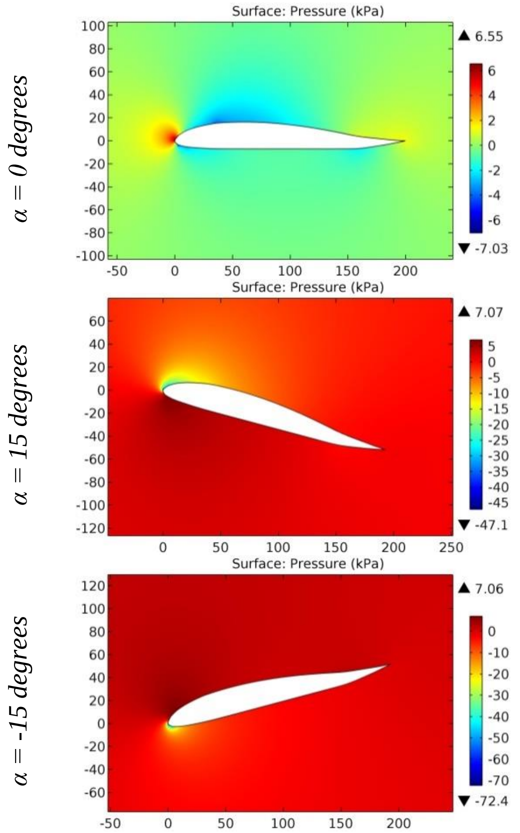

Figure 30. The pressure contours on the surfaces of the CLARK YS airfoil.

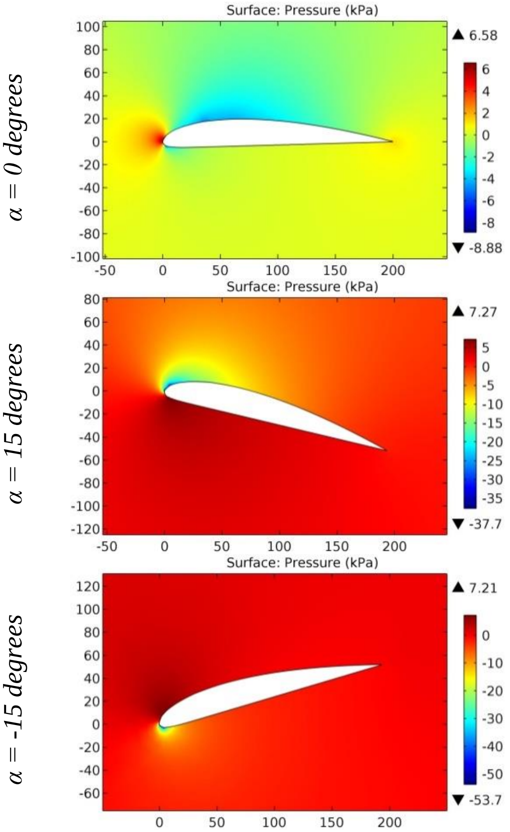

Figure 31. The pressure contours on the surfaces of the CLARK Z airfoil.

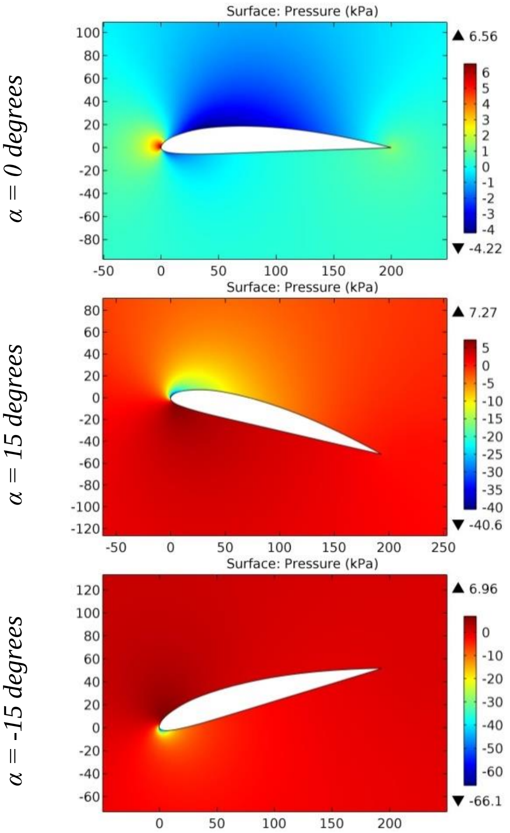

Figure 32. The pressure contours on the surfaces of the CLARK-Y 11,7% smoothed airfoil.

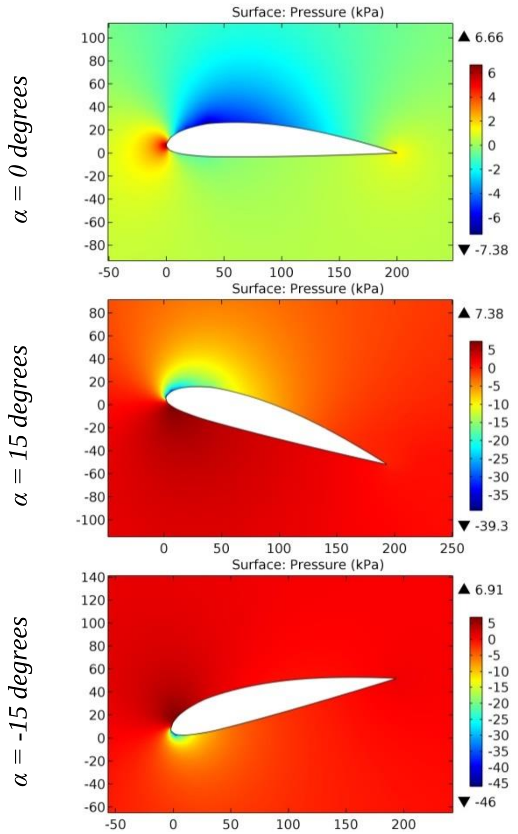

Figure 33. The pressure contours on the surfaces of the CLARKY15 airfoil.

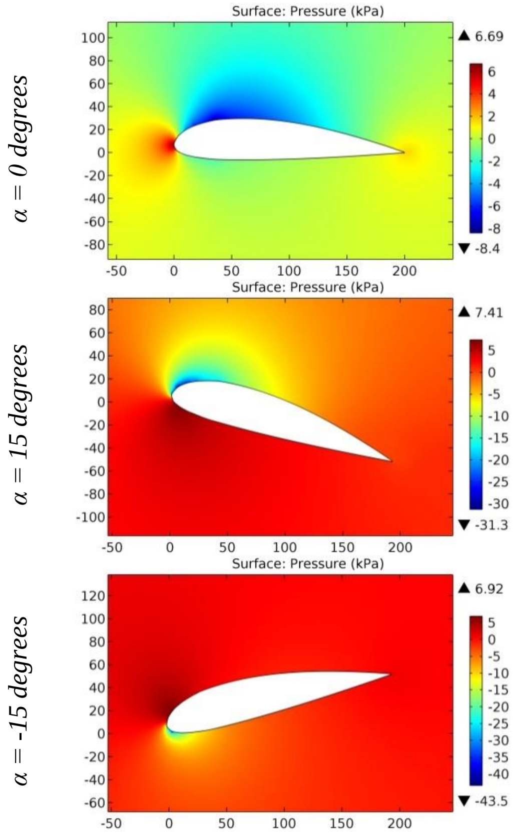

Figure 34. The pressure contours on the surfaces of the CLARKY18 airfoil.

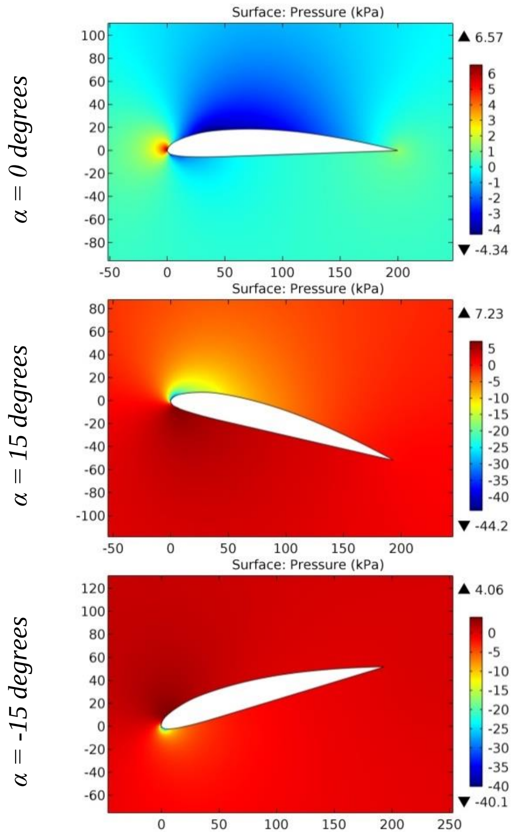

Figure 35. The pressure contours on the surfaces of the CLARK-Y2 airfoil.

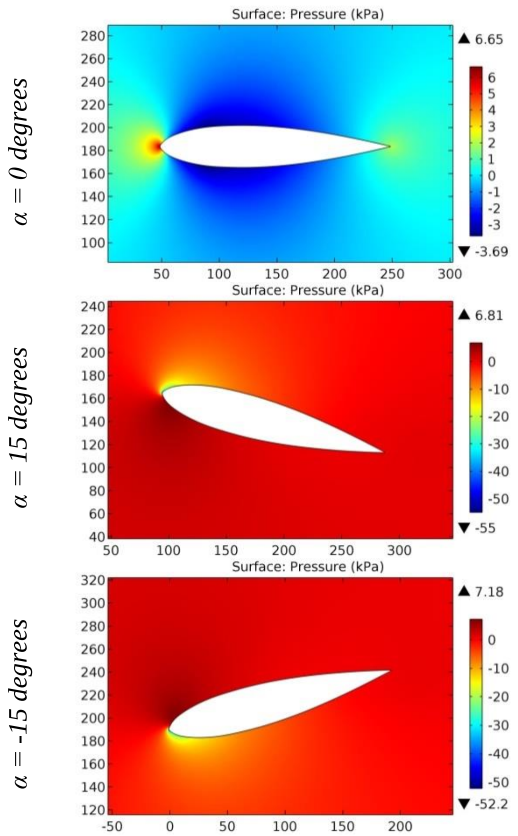

Figure 36. The pressure contours on the surfaces of the CLARKYSimm airfoil.

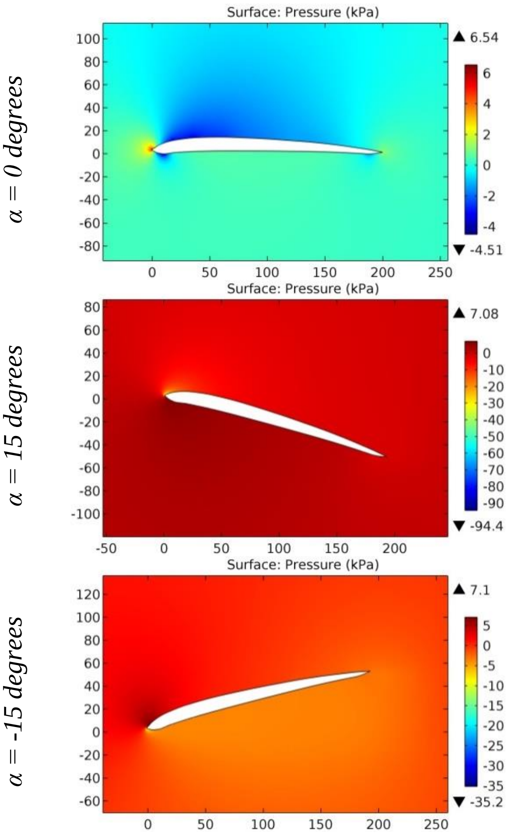

Figure 37. The pressure contours on the surfaces of the Coanda 2 airfoil.

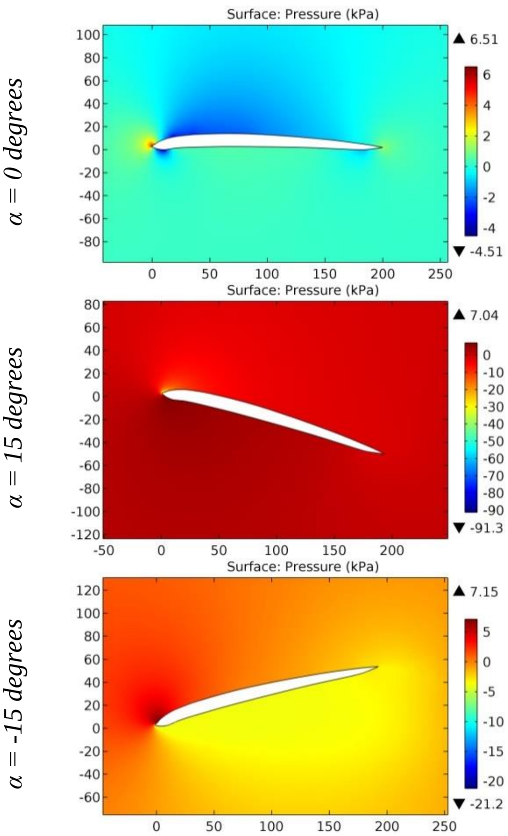

Figure 38. The pressure contours on the surfaces of the COANDA-1 airfoil.

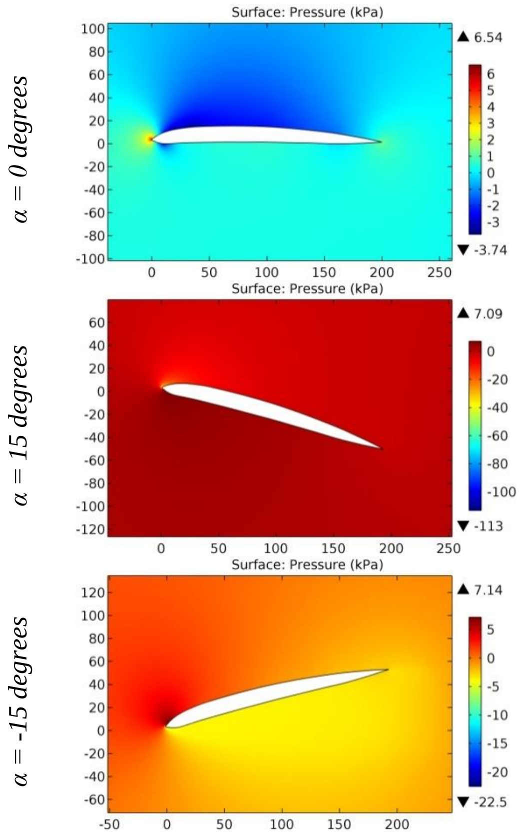

Figure 39. The pressure contours on the surfaces of the COANDA-3 airfoil.

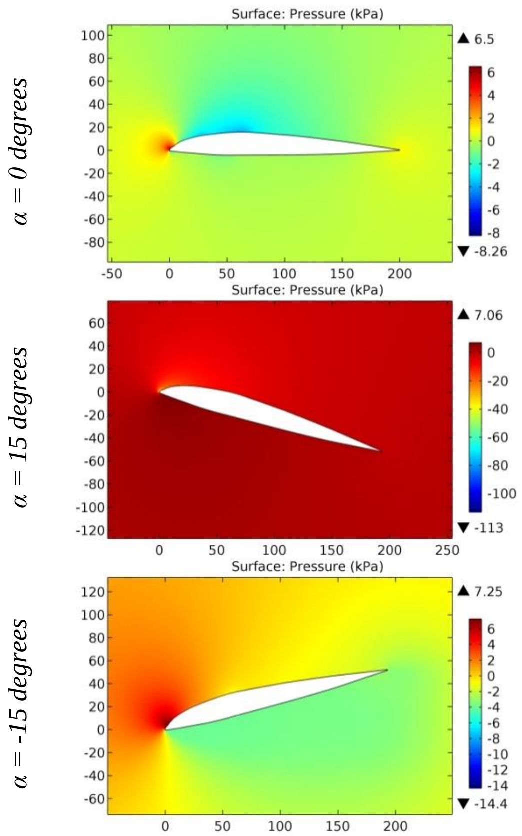

Figure 40. The pressure contours on the surfaces of the CONA airfoil.

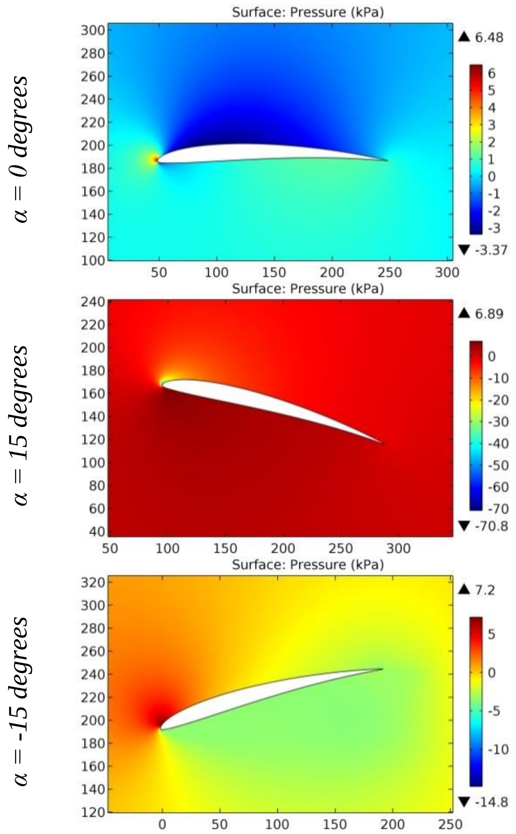

Figure 41. The pressure contours on the surfaces of the CR 001 airfoil.

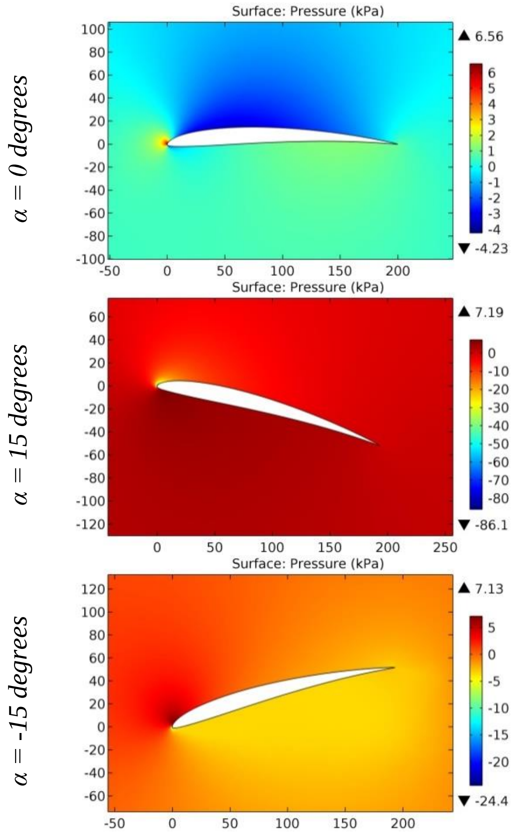

Figure 42. The pressure contours on the surfaces of the cr001sm airfoil.

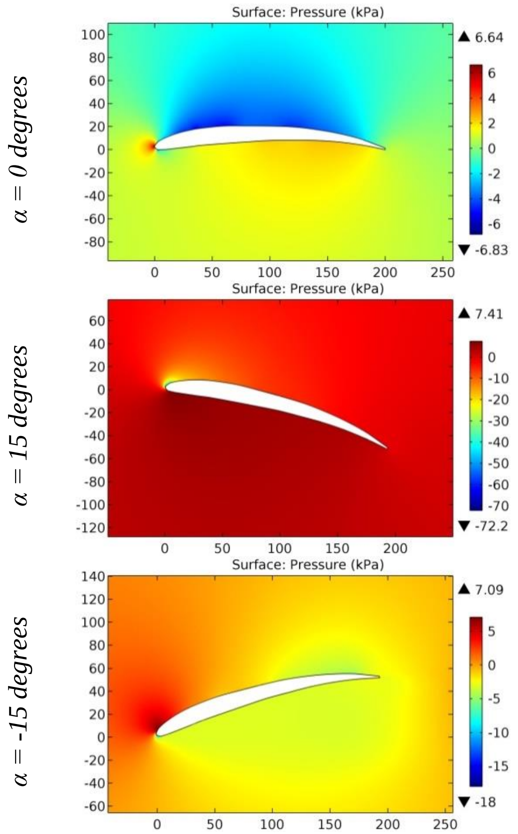

Figure 43. The pressure contours on the surfaces of the CRD-1 airfoil.

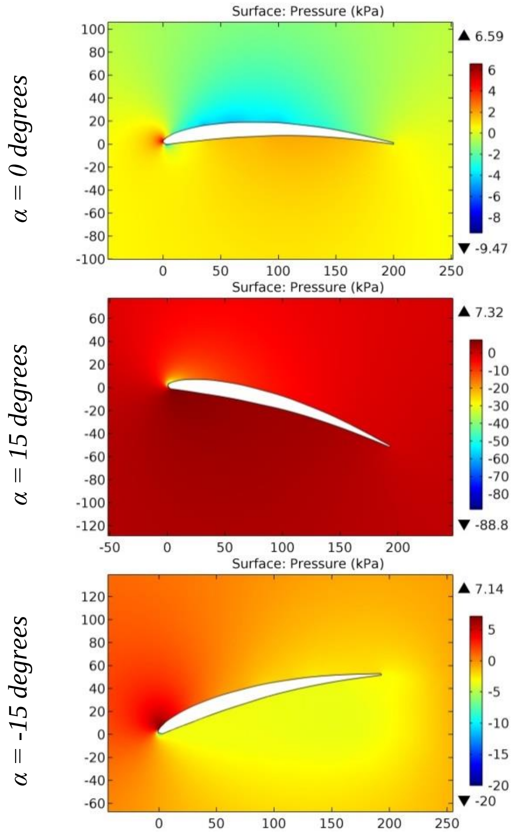

Figure 44. The pressure contours on the surfaces of the CRD-2 airfoil.

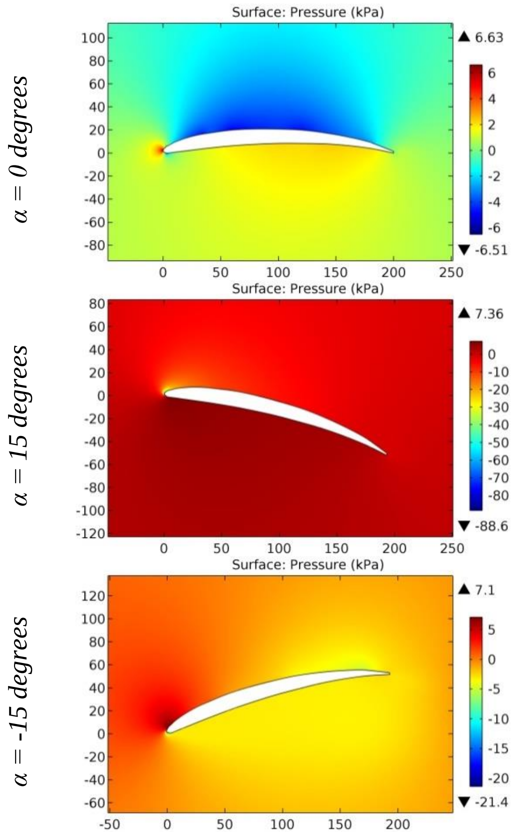

Figure 45. The pressure contours on the surfaces of the CRD-3 airfoil.

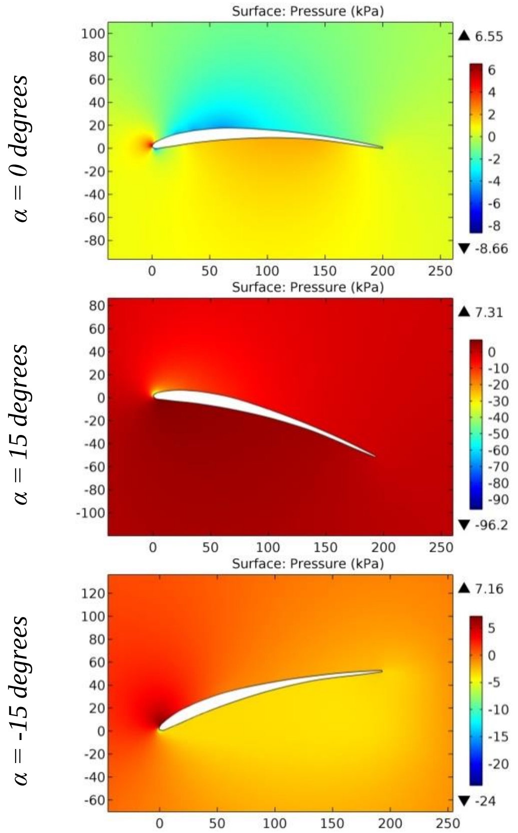

Figure 46. The pressure contours on the surfaces of the CRD-4 airfoil.

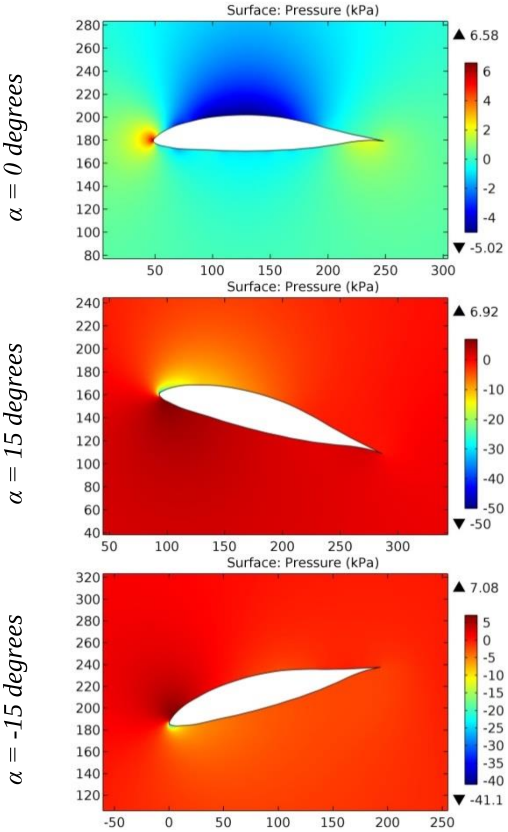

Figure 47. The pressure contours on the surfaces of the cristal cb85_15_7 airfoil.

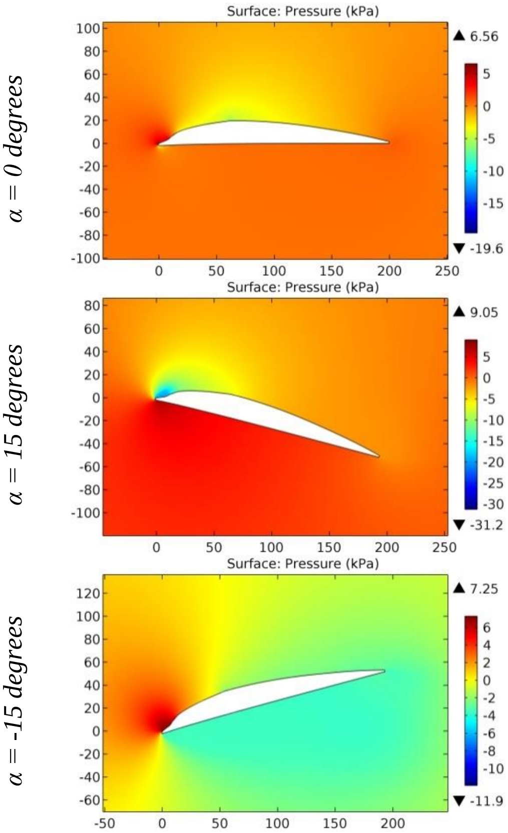

Figure 48. The pressure contours on the surfaces of the CSS airfoil.

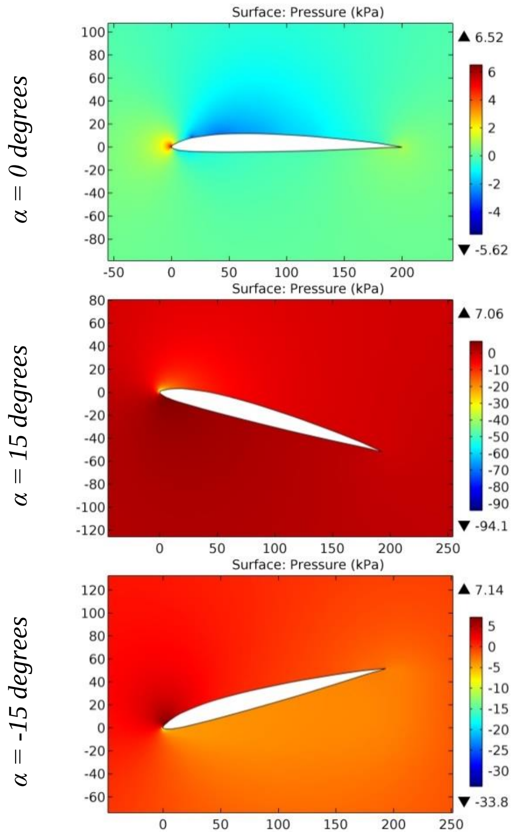

Figure 49. The pressure contours on the surfaces of the Curtiss C 62 airfoil.

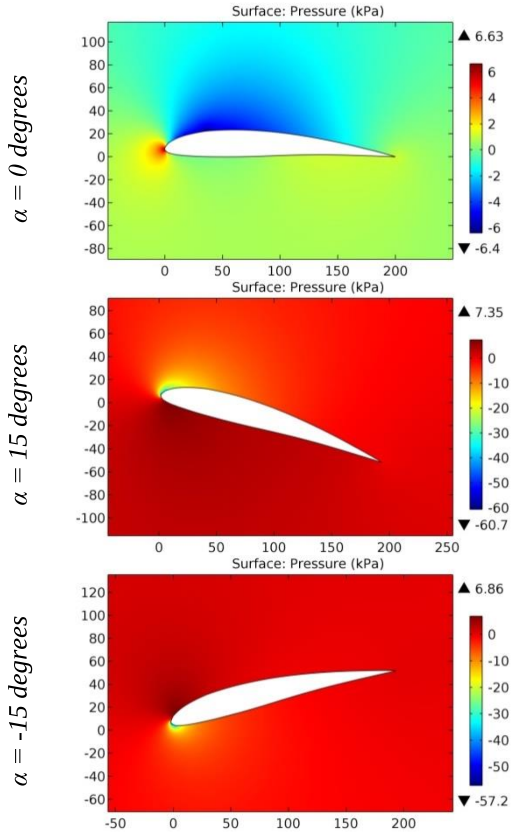

Figure 50. The pressure contours on the surfaces of the Curtiss C 72 airfoil.

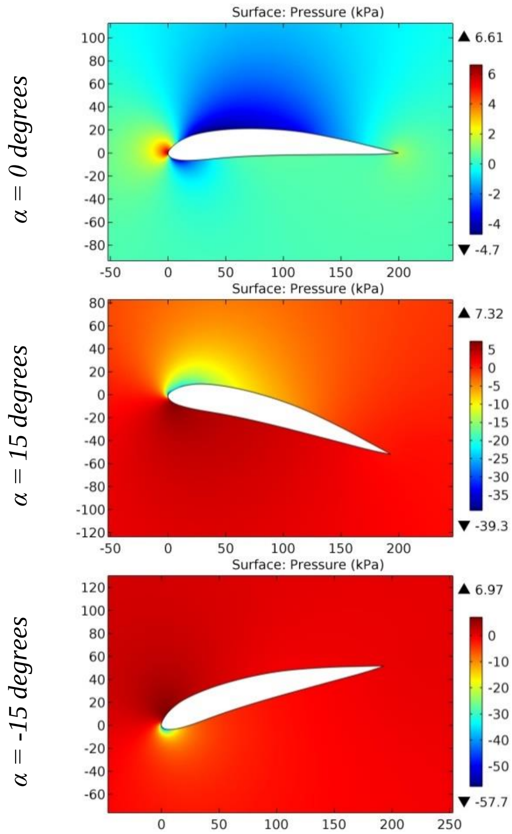

Figure 51. The pressure contours on the surfaces of the CURTISS CR-1 airfoil.

- CLARK K, CLARK V, CLARK W, CLARK X, CLARK Y, CLARK YH, CLARK YM-15, CLARK YM-18, CLARK YS, CLARK Z, CLARK-Y 11,7% smoothed, CLARKY15, CLARKY18;
- CURTISS CR-1.

The shape of the cap 21 symmetrical airfoil ensures the occurrence of the same magnitude of negative pressures on the upper and lower surfaces at the angles of attack of 15 and -15 degrees, respectively.

The maximum increase in pressure on the leading edge occurs at the angle of attack of 15 degrees for the remaining airfoils.

Conclusion

The least drag force during horizontal flight of the airplane occurs in the airfoils having the leading edge radius of 0.91%. The greatest lift force acts at the maximum thickness of the airfoil of 5.6% at 20% of the chord. These requirements are met by the CJ 2 and CAST 10-2/DOA 2 airfoils.

References:

1. Anderson, J. D. (2010). Fundamentals of Aerodynamics. *McGraw-Hill, Fifth edition*.
2. Shevell, R. S. (1989). Fundamentals of Flight. *Prentice Hall, Second edition*.
3. Houghton, E. L., & Carpenter, P. W. (2003). Aerodynamics for Engineering Students. *Fifth edition, Elsevier*.
4. Lan, E. C. T., & Roskam, J. (2003). Airplane Aerodynamics and Performance. *DAR Corp*.
5. Sadraey, M. (2009). Aircraft Performance Analysis. *VDM Verlag Dr. Müller*.
6. Anderson, J. D. (1999). Aircraft Performance and Design. *McGraw-Hill*.
7. Roskam, J. (2007). Airplane Flight Dynamics and Automatic Flight Control, Part I. *DAR Corp*.
8. Etkin, B., & Reid, L. D. (1996). Dynamics of Flight, Stability and Control. *Third Edition, Wiley*.

9. Stevens, B. L., & Lewis, F. L. (2003). Aircraft Control and Simulation. *Second Edition*, *Wiley*.
10. Chemezov, D., et al. (2021). Pressure distribution on the surfaces of the NACA 0012 airfoil under conditions of changing the angle of attack. *ISJ Theoretical & Applied Science, 09 (101)*, 601-606.
11. Chemezov, D., et al. (2021). Stressed state of surfaces of the NACA 0012 airfoil at high angles of attack. *ISJ Theoretical & Applied Science, 10 (102)*, 601-604.
12. Chemezov, D., et al. (2021). Reference data of pressure distribution on the surfaces of airfoils having the names beginning with the letter A (the first part). *ISJ Theoretical & Applied Science, 10 (102)*, 943-958.
13. Chemezov, D., et al. (2021). Reference data of pressure distribution on the surfaces of airfoils having the names beginning with the letter A (the second part). *ISJ Theoretical & Applied Science, 11 (103)*, 656-675.
14. Chemezov, D., et al. (2021). Reference data of pressure distribution on the surfaces of airfoils having the names beginning with the letter B. *ISJ Theoretical & Applied Science, 11 (103)*, 1001-1076.